Monte Carlo simulation and material growth of resonant-phonon assisted terahertz quantum cascade lasers

Yingjun Han, H. Li, Z. Y. Tan, X. G. Guo and J. C. Cao *
State Key Laboratory of Functional Materials for Informatics, Shanghai Institute of Microsystem and Information Technology, Chinese Academy of Sciences, 865 Changning Road, Shanghai 200050, P. R. China
* Email: jccao@mail.sim.ac.cn

Abstract: An ensemble Monte Carlo method is employed to evaluate the performance of resonant-phonon terahertz quantum cascade lasers. Based on our simulation, a device structure is designed to avoid the strong absorption of atmosphere. The material growth, structural analyses and optical characteristics of the laser are present. Using gold-gold waveguide layers, we demonstrate a device lasing at 3.4 *THz*, which is just located at a low-loss stage of the atmosphere.

Keywords: Terahertz, Quantum Cascade Laser, Monte Carlo

doi: 10.11906/TST.092-096.2010.06.09

1. Introduction

Recently, utilizing the active region of chirped superlattice [1], bound to continue [2] and resonant phonon [3] designs, terahertz (THz) Quantum cascade lasers (QCLs) are demonstrated as one of the most important laser sources in the applications such as THz communication and imaging. Up to now, the highest operation temperature of 186 *K* in pulse mode [4] was observed in GaAs/$Al_xGa_{1-x}As$ THz QCLs without the assistance of an applied magnetic field. At the same time, theoretical analyses have been performed by non-equilibrium Green's functions [5], rate equations [6] and Monte Carlo (MC) simulation [7]. Different scattering mechanisms [8-15] are included during the analyses of electrons transport in the devices. The output characteristics [16] and the temperature performance [15, 17, 18] of THz QCL devices are simulated and the influences of the modifications of devices' structure [19] and growth parameters [20] are explored.

In this paper, we use a MC method to investigate the device performance of a THz QCL, such as current-voltage characteristics and the evolution of optical mode gain. Based on our simulation, a proper lasing frequency is selected to avoid the strong absorption of atmosphere.

2. Theoretical model

In our simulation, 5000 electrons are engaged in three modules of devices according to an ensemble MC model. We assume that the individual modules are ideally periodic. An electron scattered out of a module is reinjected with identical in-plane wave vector. Electron-LO phonon (e-LO) and electron-electron (e-e) scattering are included in the simulation. Due to the low Al composition, only bulk GaAs phonon mode is considered as a good approximation. Self scattering technique [21] and a simplified multi-subband screening mode [22] are used to deal with the scattering between two electrons. To avoid introducing artificial error by random

selection of the partner electron, the maximum electron-electron scattering probability is modified in our model [20]. The Pauli exclusion principle is applied to deal with the degeneracy effect. The lattice temperature is set to 25 *K* and no phenomenal parameters are introduced in the simulation.

3. Simulation results

The simulated device structures are based on GaAs/AlGaAs material system which is grown by molecular beam epitaxy (MBE). Fig. 1 shows the conduction band diagrams of four-well resonant-phonon THz QCL. Starting from the injection barrier, the layer sequences are 5.3/7.6/2.3/6.2/3.7/14.9/3.4/8.6 *nm*, where the barrier layers are shown in bold and the doped layer ($2.36\times10^{16}\ cm^{-3}$) is underlined. Radiative transition takes place vertically from subband 5 to subband 4 with the dipole matrix element of 5.5 *nm*. The depopulation process is assisted by resonant phonons, making sure of a short carrier lifetime of subband 4 and hence the population inversion. The devices are fabricated according to the gold-gold waveguide process outlined in Ref. 23 and a laser ridge of $100\mu m\times1mm$ is used in the calculation of waveguide and mirror loss.

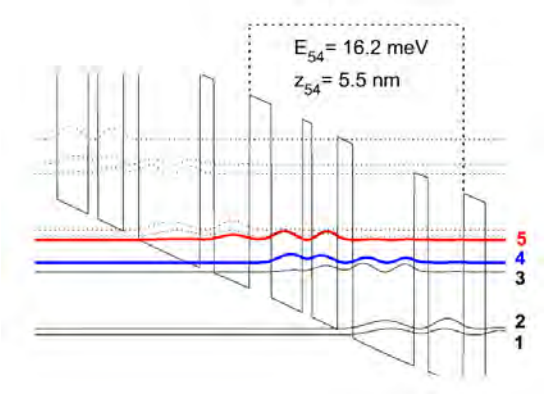

Fig.1 Calculated potential profile and squared wavefunctions of the THz QCL. The external applied bias is 68 *mV*/module.

The calculated current density as a function of applied bias is shown in Fig. 2. With a serial resistance of 1.2 ohm in the circuit, the calculated current-voltage characteristic is in good agreement with the measured one. When the bias is near the designed value, the current increases rapidly and population inversion is achieved for lasing operation. If the bias increases further, the current will decrease because the resonance between subband 5 and 1' (the injection subband) is broken. At the applied bias around 8.5*V*, the calculated current is much larger than the measured one, which is omitted in the figure and has been attributed to the overestimation of a parasitic coupling duo to the neglect of dephasing effects [24]. The optical gain is related with $\Delta n_{54} f_{54} (\Delta\nu)^{-1}$, where Δn_{54} is the population inversion, f_{54} is the oscillation strength and $\Delta\nu$ is the spontaneous emission linewidth. Waveguide loss is analyzed using an effective index method and the permittivity of materials is calculated based on the Drude model. The calculated optical gain is compared with the threshold gain. As a measured $\Delta\nu$ of 1.03 *THz* is used, the lasing domain can be estimated at the bias from 12.1 *V* to 15.0 *V*, which is a little smaller than the experiment results (from 12.8 *V* to 17.0 *V*). Because there is a shift between the curve of Δn_{54} and f_{54}, two peaks are observed for the optical gain which is the possible reason for the enhancement of laser

intensity observed in the experiment at bias of 16*V* [25]. Our results show that the MC simulation is a useful method to investigate the electronic transportation in THz QCLs.

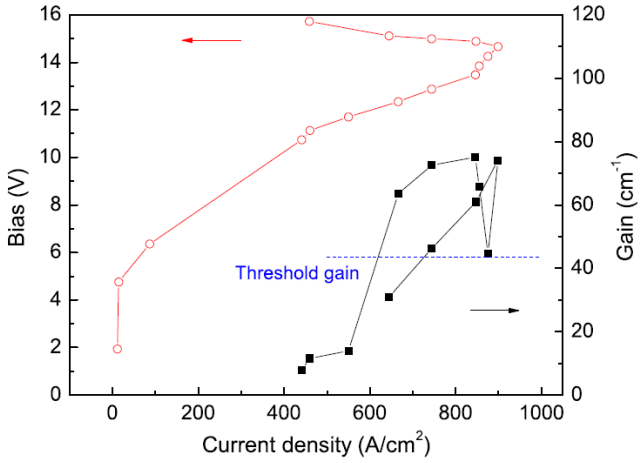

Fig.2 The calculated current-voltage and current-gain characteristics of the THz QCL. The current is overestimated at the bias of 8.5 *V* in the calculations, which has been omitted in the figure.

4. Experiment results

The THz QCL sample was grown by gas-source molecular beam epitaxy (GSMBE, VG90) on a semi-insulating GaAs (001) substrate. As the group V source, arsine (AsH_3) was cracked into As_2 at temperature of 1000 ℃ and its flux was controlled by a Baratron pressure gauge. The active region of THz QCL consists of 176 modules described above and the growth sequences were 800 *nm* GaAs buffer layer, 100 *nm* AlAs etch-stop layer, 98 *nm* GaAs:Si (5×10^{18} cm^{-3}), the active region, 58 *nm* GaAs:Si (5×10^{18} cm^{-3}) and 3.5 *nm* LT-GaAs layer. The growth temperature was 600 ℃ for the active region and the growth rate was 975 *nm/h* for GaAs and 176.5 *nm/h* for AlAs, respectively.

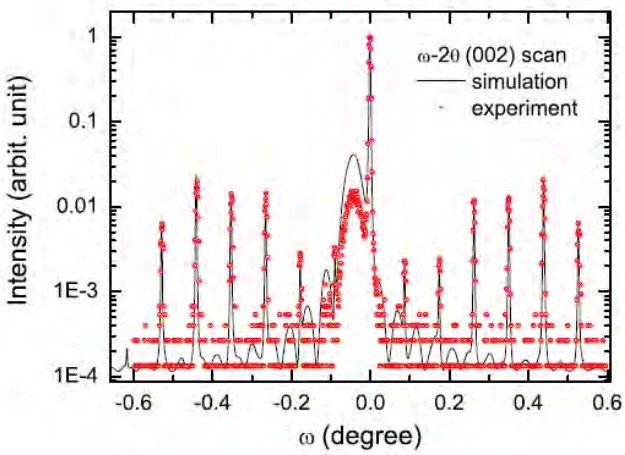

Fig.3 GaAs (002) ω-2θ XRD scans of THz QCL structure. The measured and simulated results are indicated by scatters and a line, respectively.

After growth, structural characteristics were carried out by high-resolution X-ray diffraction (HRXRD). Fig. 3 shows the GaAs (002) ω-2θ XRD spectrum of the sample and a theoretical simulation curve for the structure with design parameters. The measured results are in good agreement with the simulated curve, which indicates that the growth process is well controlled and the structure has a good quality.

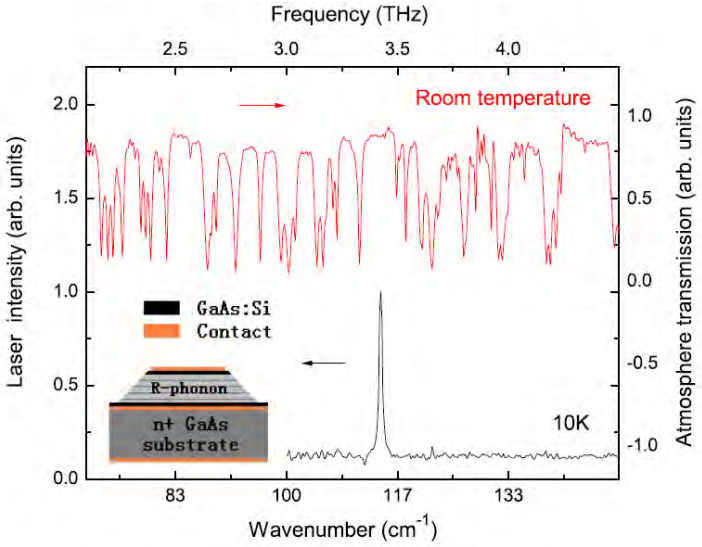

Fig.4 THz QCL emission spectrum measured at 10*K* and room temperature atmosphere transmission spectrum with a measured humidity of 51%. The inset figure shows the device structure with a metal-metal waveguide.

The devices are fabricated with Au-Au waveguide structure [23]. To facilitate the electrical and optical measurements at cryogenic temperatures, the devices are attached to a copper heat sink and the temperature can be changed from 10 *K* to room temperature by a closed cycle helium cryostat. Devices are tested in pulsed mode powered by an AVTECH pulse generator with 5 μs pulses at a 2 *kHz* repetition rate (1% duty cycle) and THz spectra are measure by a Fourier Transfer spectrometer (Bruker v60s) with a Mylar beam splitter and a DTGS-PE detector included. As shown in Fig. 4, under the bias of 14.8 *V*, the lasing frequency is 3.4 *THz* at 10*K*, which is just located at a low-loss stage of atmosphere. Therefore, such a device can be used for the optical communication or imaging which is performed in the atmosphere.

5. Conclusions

An MC simulation is used to investigate the electric and optical properties of THz QCLs. The calculated current-voltage characteristics and the evolution of optical gain are in agreement with the experiment results. THz QCL samples are grown by MBE and the device is operated at 3.4 THz which is just located at a low-loss stage of the atmosphere.

Acknowledgement

Authors would like to thank Prof. H. C. Liu for his help in the devices fabrication. This work was supported by the National Basic Research Program of China (Project No. 2007CB310402),

the National Natural Science Foundation of China (Project Nos. 60721004 and 60606027), and the major project (KGCX2-YW-231) and "Hundred Scholar Plan" of the Chinese Academy of Sciences.

References

[1] R. Köhler, A. Tredicucci, F. Beltram, H. E. Beere, E. H. Linfield, A. G. Davies, D. A. Ritchie, R. C. Iotti, and F. Rossi, *Nature*, 417, 156, (2002).

[2] G. Scalari, L. Ajili, J. Faist, H. Beere, E. Linfield, D. Ritchie, and G. Davies, *Appl. Phys. Lett.*, 82, 3165, (2003).

[3] B. S. Williams, H. Callebaut, S. Kumar, Q. Hu, and J. L. Reno, *Appl. Phys. Lett.*, 82, 1015, (2003).

[4] S. Kumar, Q. Hu, and J. L. Reno, *Appl. Phys. Lett.*, 94, 131105, (2009).

[5] S. -C. Lee and A. Wacker, *Phys. Rev. B*, 66, 245314, (2002).

[6] D. Indjin, P. Harrison, R. W. Kelsall, and Z. Ikonić, *J. Appl. Phys.*, 91, 9019, (2002).

[7] C. Jacoboni and L. Reggiani, *Rev. Mod. Phys.*, 55, 645, (1983).

[8] S. M. Goodnick and P. Lugli, *Phys. Rev. B*, 37, 2578, (1988).

[9] O. Bonno, J. L. Thobel, and F. Dessenne, J. Appl. Phys., 97, 043702, (2005).

[10] J. T. Lü and J. C. Cao, *Appl. Phys. Lett.*, 88, 061119, (2006).

[11] H. Callebaut, S. Kumar, B. S. Williams, Q. Hu, and J. L. Reno, *Appl. Phys. Lett.*, 84, 645, (2004).

[12] N. Regnault, R. Ferreira, and G. Bastard, *Phys. Rev. B*, 76, 165121, (2007).

[13] T. Li, R. P. Joshi, and C. Fazi, *J. Appl. Phys.*, 88, 829, (2000).

[14] H. Callebaut, S. Kumar, B. S. Williams, Q. Hu, and J. L. Reno, *Appl. Phys. Lett.*, 83, 207, (2003).

[15] D. Indjin, P. Harrison, R. W. Kelsall, and Z. Ikonić, *Appl. Phys. Lett.*, 82, 1347, (2003).

[16] H. Li, J. C. Cao, and J. T. Lü, J Appl. Phys. 103, 103113, (2008).

[17] C. Jirauschek and P. Lugli, Phys. Status Solidi C 5, 1610, (2008).

[18] J. C. Cao, J. T. Lu, and H. Li, Physica E 41, 282, (2008).

[19] H. Li, J. C. Cao, J. T. Lü, and Y. J. Han, Appl. Phys. Lett. 92, 221105, (2008).

[20] Yingjun Han and J. C. Cao, *Semicond. Sci. Tech.*, 24, 095026, (2009).

[21] S. M. Goodnick and P. Lugli, *Phys. Rev. B*, 37, 2578, (1988).

[22] O. Bonno, J. L. Thobel, and F. Dessenne, *J. Appl. Phys.*, 97, 043702, (2005).

[23] B. S. Williams, S. Kumar, H. Callebaut, Q. Hu, and J. L. Reno, *Appl. Phys. Lett.*, 83, 2124, (2003).

[24] H. Callebaut and Q. Hu, *J. Appl. Phys.*, 98, 104505, (2005).

[25] J. C. Cao, H. Li, Y. J. Han, Z. Y. Tan, J. T. Lü, H. Luo, S. Laframboise, and H. C. Liu, *Chinese Phys. Lett.*, 25, 953, (2008).